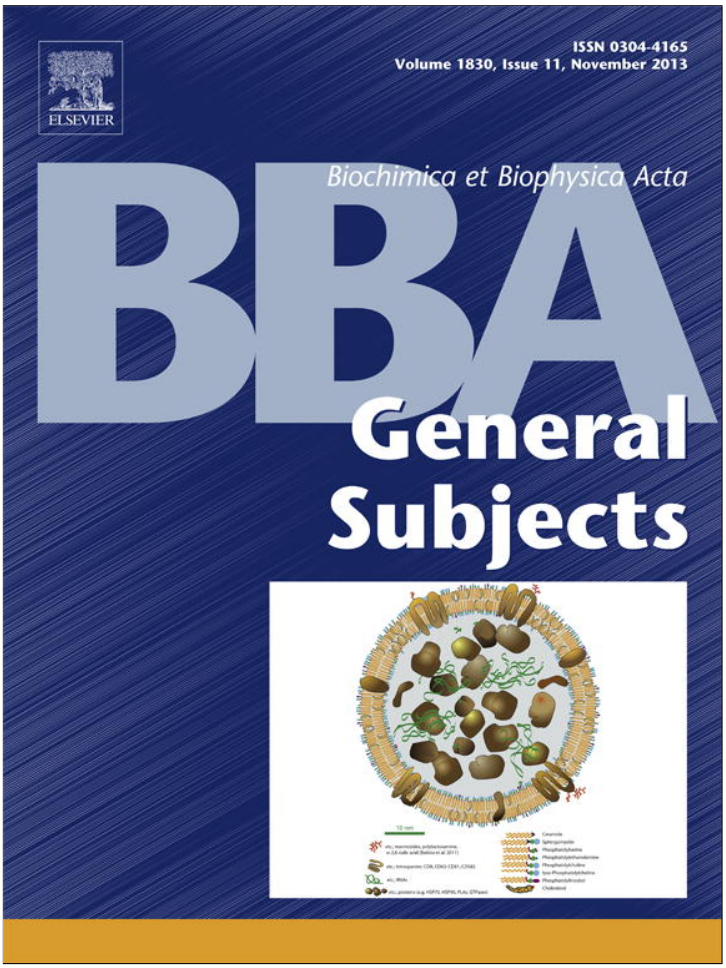

Biochimica et Biophysica Acta 1830 (2013) 5036–5048

Contents lists available at ScienceDirect

Biochimica et Biophysica Acta

journal homepage: www.elsevier.com/locate/bbagen

Structural and functional differences between pheromonotropic and melanotropic PK/PBAN receptors

Aliza Hariton-Shalev [a], Moran Shalev [b], Noam Adir [c], Edurad Belausov [d], Miriam Altstein [a,*]

[a] Department of Entomology, The Volcani Center, Bet Dagan 50250, Israel
[b] The Edith and Joseph Fischer Enzyme Inhibitors Laboratory, Schulich Faculty of Chemistry, Technion—Israel Institute of Technology, Haifa 32000, Israel
[c] Schulich Faculty of Chemistry, Technion—Israel Institute of Technology, Haifa 32000, Israel
[d] Institute of Plant Sciences, The Volcani Center, Bet Dagan 50250, Israel

ARTICLE INFO

Article history:
Received 15 January 2013
Received in revised form 17 June 2013
Accepted 29 June 2013
Available online 10 July 2013

Keywords:
Insect neuropeptide
Pheromone biosynthesis-activating neuropeptide-receptor
Diapause hormone
Heliothis peltigera
Spodoptera littoralis

ABSTRACT

Background: The pyrokinin/pheromone biosynthesis-activating neuropeptide (PK/PBAN) plays a major role in regulating a wide range of physiological processes in insects. The ubiquitous and multifunctional nature of the PK/PBAN peptide family raises many questions regarding the mechanisms by which these neuropeptides elicit their effects and the nature of the receptors that mediate their functions.
Methods: A sex pheromone gland receptor of the PK/PBAN family from *Heliothis peltigera* female moth and a *Spodoptera littoralis* larval receptor were cloned and stably expressed, and their structural models, electrostatic potentials and cellular functional properties were evaluated.
Results: Homology modeling indicated highly conserved amino-acid residues in appropriate structural positions as experimentally shown for class A G-protein coupled receptors. Structural differences could be proposed and electrostatic potentials of the two receptor models revealed net charge differences. Calcium mobilization assays demonstrated that both receptors were fully functional and could initiate extracellular calcium influx to start PK/PBAN signal transduction. Evaluation of the signaling response of both receptors to PBAN and diapause hormone (DH) revealed a highly sensitive, though differential response. Both receptors responded to PBAN whereas only *Spl*-PK/PBAN-R exhibited a high response toward DH.
Conclusions: The structural, electrostatic and cellular functional differences indicate that different PK/PBAN in vivo functions may be mediated by different PK/PBAN receptors and elicited by different peptide(s).
General significance: The results advance our understanding of the mode of action of the PK/PBAN family, and might help in exploring novel high-affinity receptor-specific antagonists that can serve as a basis for the development of new families of insect-control agents.

1. Introduction

The pyrokinin/pheromone biosynthesis-activating neuropeptide (PK/PBAN) family is one of the most studied neuropeptide (Np) families in insects, and one of the most important in regulating their physiology. The family is ubiquitous and multifunctional, and plays major roles in regulating a wide range of developmental processes, feeding, mating and behavior [1,2]. The family comprises the following C-terminally amidated peptides: PKs, PBANs, diapause hormone (DH), β- and γ-subesophageal Nps (SGNPs) and some myotropins (MTs), all of which share a common C-terminal sequence (FXPRLa). PK/PBAN peptides are encoded by two genes: *pban* gene, which in moths encodes five peptides, four of which contain the C-terminal consensus sequence FXPRLa (PBAN, DH, β- and γ-SGNPs); and *capa* gene, which encodes three peptides, one of which – a DH-like peptide (termed herein CAPA-DH) – is a member of the family. To avoid terminological confusion, in the present paper we refer to the individual peptides as *pban*-gene-encoded peptides or *capa*-gene-encoded peptides and to all the FXPRLa-containing peptides as the PK/PBAN family. For a review on the PK/PBAN peptides see [1,3].

The ubiquitous and multifunctional nature of the PK/PBAN peptide family raises many questions regarding the mechanisms by which these Nps elicit their effects in different insects, the nature of the receptors that mediate these function, and also the nature of the receptor/ligand interactions and their translation to downstream cellular signaling. Indeed, in the past decade a vast amount of information has been gained on the PK/PBAN receptors (PK/PBAN-Rs) and their signaling cascade. Similar to other Nps, the PK/PBAN Nps activate cellular processes via G-protein-coupled receptors (GPCRs) [3] located on the

Abbreviations: CAPA-DH, *capa*-gene-derived peptide; DH, diapause hormone; ECL, extra-cellular loop; GPCR, G-protein-coupled receptor; ICL, intra-cellular loop; Np, neuropeptide; PI, pre-immune serum; PK/PBAN, pyrokinin/pheromone biosynthesis-activating neuropeptide; PK/PBAN-R, PK/PBAN receptor; SGNPs, β- and γ-subesophageal Nps

* Corresponding author at: Department of Entomology, The Volcani Center, P.O. Box 6, Bet Dagan 50250, Israel. Tel.: +972 3 968 3710; fax: +972 3 968 3835.
E-mail address: vinnie2@agri.gov.il (M. Altstein).

0304-4165/$ – see front matter © 2013 Elsevier B.V. All rights reserved.
http://dx.doi.org/10.1016/j.bbagen.2013.06.041

surface of the Nps' target cells [4]. In the past decade many PK/PBAN-Rs have been cloned from *Drosophila melanogaster*, *Anopheles gambiae*, pheromone glands of adult female moth species (e.g., *Helicoverpa zea*, *Bombyx mori*, *Heliothis virescens*, *Helicoverpa armigera*, *Plutella xylostella*, *Spodoptera exigua* and *Pseudoletia separata*), moths larvae (e.g., *Spodoptera littoralis* and *H. virescens*) and *B. mori* pupa [1,5–8]. The occurrence of a PK/PBAN-R in adult male moths has also been reported [9].

More detailed studies have recently revealed the presence of multiple isoforms or variants of PK/PBAN-Rs of the moth pheromone gland in *H. virescens*, *B. mori*, *H. armigera*, *H. zea*, *P. separata* and *Manduca sexta* which differ in having a "long" or a "short" C-terminal tail, and arise from alternative splicing [8,10]. To date, 28 PK/PBAN-Rs including the different variants, have been cloned from various insects, and most of them were transiently or stably expressed in diverse expression systems, e.g., insect or mammalian cell lines or *Xenopus* oocytes. Another 16 were annotated according to sequence homologies with previously cloned PK/PBAN-Rs or predicted sequences [1,5]. Pending their full characterization, the receptors in the present study are referred to by the general term: PK/PBAN-R and are designated according to terminology suggested by Raina and Gade for insect Nps [11] (e.g., *Drm*-Rs for *D. melanogaster* receptor).

Many of the actually cloned receptors have been identified, mainly by their ability to elicit Ca flux in response to stimulation with various PK/PBAN ligands. Most studies on the signaling cascade of PK/PBAN-Rs used lepidopteran sex pheromone gland receptors. In all moth species tested so far Ca^{2+} was found necessary for biological response and activation of the PK/PBAN-Rs by ligands resulted in an influx of extracellular calcium and a subsequent increase in cytosolic Ca^{2+}. Depletion of Ca^{2+} caused loss of pheromonotropic activity [12]. Although extracellular Ca^{2+} has proved absolutely necessary for the bioactivity of PBAN in all moth species tested so far, the Np-stimulated intracellular signal transduction cascade differed among moth species [12,13].

Although much progress has been made on characterization of the PK/PBAN-Rs, most studies focused on their differing affinities toward *capa*- or *pban*-gene-derived ligands, and downstream signaling; very little attention was paid to correlation of the various receptor–ligand interactions with the in vivo functions they mediate. This issue is of major importance, especially in view of the multifunctional nature of this family of Nps. Currently, it is still not clear which receptor(s) mediate each of the in vivo functions elicited by the PK/PBAN peptide family; we still do not know whether each function is mediated by a single or multiple receptor(s), or whether each function is elicited by one or more PK/PBAN peptides. Even our knowledge of the interaction of the PK/PBAN peptides with the receptor is still limited, as is our understanding of the receptors' structure/activity relationship. All of the above issues require further investigation and need to be examined with respect to each in vivo function.

In a previous study we used in vivo pheromonotropic and melanotropic assays (with *H. peltigera* and *S. littoralis* moth, respectively) to study the structure/activity relationship of a large variety of PK/PBAN peptides and their analogs and to determine whether the two functions were meditated by different PK/PBAN-Rs which respond to the different peptides. For this purpose, we used conformationally constrained backbone cyclic PK/PBAN agonists and antagonists, which exhibit high receptor selectivity [14]. These studies yielded strong indications of the existence in *H. peltigera* and *S. littoralis* of different PK/PBAN-Rs, which mediate sex pheromone biosynthesis in the pheromone gland and cuticular melanization in moth larvae, respectively [15]. In the present study we cloned and stably expressed the *H. peltigera* pheromone gland receptor in *Spodoptera frugiperda* (*Sf9*) cells, and compared it with our previously cloned *S. littoralis* larval receptor (also expressed in *Sf9* cells), with respect to their structure, electrostatic potentials and cellular functional properties (i.e., induction of Ca^{2+} flux) in response to their stimulation with various ligands, in an attempt to identify differences between the two PK/PBAN-Rs that mediate two different in vivo functions.

2. Materials and methods

2.1. Peptides

Synthetic *Hez*-PBAN (based on the sequence of *H. zea*, *Hez*-PBAN 1–33-amide) and *Spl*-DH (based on the sequence of *S. littoralis* DH) were synthesized with an ABI 433A automatic peptide synthesizer on Rink amid MBHA resin by means of the FastMocTM chemistry as described previously [16].

2.2. Insects

H. peltigera moths were reared on an artificial diet as described previously [17]. Pupae were sexed and females and males were placed in separate rooms with a dark/light regime of 10/14 h, at 25 ± 2 °C and 60–70% relative humidity. Adult moths were kept in screen cages and supplied with a 10% sugar solution. Moth populations were refreshed every year with males caught from the wild by means of pheromone traps, as described previously [17]. All females used in this study were 2–3 days old.

2.3. Cell lines

The *S. frugiperda* pupal ovarian cell line (*Sf9*) [18] was cultured at 27 °C in 4 ml of Grace's Medium (Biological Industries, Beit-Haemek, Israel) supplemented with 10% heat-inactivated fetal bovine serum, 1% Lactalbumin, 1% Yeastolate (all supplied by Biological Industries and termed herein complete Grace's insect medium) in 25-cm^2 flask (Corning, NY, USA). Cell passage was carried out every 3–4 days.

2.4. H. peltigera receptor cloning

The pheromone glands of 2- to 3-day-old *H. peltigera* females were excised and immediately frozen at −80 °C pending use. Total RNA was isolated from the pheromone glands with TRIzol (Invitrogen, Carlsbad, CA, USA). The quality and quantity of the RNA were assessed with a NanoDrop ND-100 spectrophotometer (Thermo Fisher Scientific, Wilmington, DE, USA). Poly(A)$^+$ RNA was isolated from 100 μg of total RNA with the Oligotex Direct mRNA Isolation Kit (Qiagen, Hilden, Germany) according to the manufacturer's instructions, and was then subjected to a reverse-transcription reaction, carried out with an Omniscript Reverse Transcription Kit (Qiagen) according to the manufacturer's instructions, starting with 2 μg of RNA for a single reaction. The PCR reactions were carried out with gene-specific primers (for details see Results section) with: 50 ng of DNA template; 0.5 μl (10 mM) of each primer (IDT, Jerusalem, Israel); 0.2 μl of Pfu DNA Polymerase, 2.5 μl of Pfu buffer and 0.5 μl of dNTP mix (each at 2.5 mM) and 2.5 mM $MgCl_2$ (all supplied by Fermentas, Thermo Scientific, Burlington, Canada). Reactions were carried out with a Multigene Gradient PCR thermal cycler (Labnet International, Woodbridge, NJ, USA) as follows: 1 cycle of 94 °C for 5 min, 29 cycles of 94 °C for 30 s and 57 °C for 30 s, followed by a final step of 72 °C for 1 min. Following determination of the sequences of the 5′ and 3′ untranslated regions (UTRs) of this gene at the Center of Genomic Technologies of the Hebrew University of Jerusalem, Israel, sequences were assembled and an open reading frame (ORF) of 1029 base pairs was predicted with the SIB ExPASy Bioinformatics Resource portal.

2.5. Vector construction, sub-cloning, propagation and insert characterization

2.5.1. H. peltigera

A new set of primers was designed in order to obtain two restriction sites on the cloned gene, one at each end of the sequence. In addition, in order to enhance expression of this gene in the cells, we

designed a partially mismatched primer that would insert an ideal Kozak signal GCCACC [19] immediately before the start-codon ATG. The designed primers were: 5′-AGGAGAGGATCCGCCACCATGACA-3′ (BamHI — 5′-G^GATCC-3′) and 5′-AGGAGATCTAGATCACCTTGAA GGCGT-3′ (XbaI — 5′-T^CTAGA-3′). A PCR reaction was carried out as in Section 2.4, with an annealing temperature of 63 °C and 3 mM of $MgCl_2$. The PCR product was subjected to 1% agarose gel electrophoresis, purified by means of a Wizard SV Gel clean-up system (Promega, Madison, WI, USA), ligated into *pGEM* cloning vector (Promega), and propagated in DH5α *Escherichia coli*-competent cells (Bio-Lab, Jerusalem, Israel) by using the following protocol: a 100-μl vial of competent cells was thawed on ice and 1 μl of DNA was added to it. The vial contents were mixed gently and the vial was placed on ice for another 20 min. The reaction mixture was transferred to 42 °C for 45 s and then cooled on ice for 2 min. Competent cells were transferred to 15-ml tubes containing 950 μl of Lysogeny Broth (LB) medium (LB Broth type BP302/400s; Hy-lab Ltd., Rehovot, Israel) and placed in a shaking incubator at 250 rpm for 1 h at 37 °C. Aliquots of 100 μl of transformed bacteria suspension were plated on LB agar plates containing Ampicillin at 100 μg/ml (Ampicillin-Duchefa, Haarlem, the Netherlands) onto which 20 μl of X-gal (Ornat, Rehovot, Israel) at 50 mg/ml and 100 μl of 0.1 M isopropyl-β-D-thiogalactopyranoside (Ornat) were spread. The culture was screened for white colonies (which contained the insert). DNA was extracted from the white colonies with the QIAamp DNA purification kit (Qiagen) and, in order to obtain sticky ends, 20 μl, i.e., 800 ng, of the construct *pGEM*-insert was digested with 1.5 μl (10 U/μl) of BamHI (Fermentas) in a reaction mixture that contained 4 μl of double-distilled water (DDW) and 3 μl of Tango Buffer (Fermentas), incubated at 37 °C for 1.5 h, and then heat-inactivated at 80 °C for 20 min. After inactivation 1.5 μl (10 U/μl) of XbaI (Fermentas) were added to the same reaction mixture, which was then incubated at 37 °C for another 1.5 h. Aliquots of 1000 ng of pIZ/V5-His (Invitrogen) were propagated in DH5α *E. coli*-competent cells as described above (this section) and digested with the same restriction enzymes under the same conditions.

Aliquots, each of 100 ng, of PK/PBAN-R insert and of pIZ/V5-His were ligated by means of T4 DNA ligase (Promega). The reaction mixture was incubated with 2 μl of 10× Ligase buffer and 3 units, i.e., 1 μl, of T4 ligase in a total volume of 20 μl for 3 h at room temperature (RT). Three colonies were selected, the pIZ/V5-His containing the PK/PBAN-R insert was extracted with the QIAamp DNA purification kit (Qiagen), subjected to PCR as described above (this section), with 2.5 mM $MgCl_2$, and re-sequenced by the Center of Genomic Technologies, prior to its transfection into cells. The resulting PCR products yielded identical sequences for the ORFs.

2.5.2. S. littoralis

Spl-PK/PBAN-R has been previously cloned by us [20]. In order to generate stable expression of the gene in *Sf9* cells it was necessary to transfer the gene from pCR2.1 cloning vector to pIZV5-His expression vector. The *Spl*-PK/PBAN-R gene was first excised from the plasmid as follows: One microliter of DNA (200–300 ng of pCR2.1 cloning vector containing the *Spl*-PK/PBAN-R insert) was incubated for 1 h in a dry bath at 37 °C with 0.8 μl (10 U/μl) of HindIII, 0.8 μl (10 U/μl) of XhoI, and 1.5 μl of Rx10 Buffer (all purchased from Fermentas, Thermo Scientific) and 11.7 μl of DDW. The gene was purified with 1% agarose gel and subjected to a PCR reaction with 10 ng of DNA template, 0.5 μl of each primer (see below, this section) at 10 mM (IDT, Jerusalem, Israel), 0.4 μl of 2.5 mM i-Pfu enzyme, 2.5 μl of 2.5 mM i-Pfu buffer, 0.5 μl of 2.5 mM dNTP mix and 2.5 mM $MgCl_2$ (all supplied by Intron, Korea). The primers used were designed to amplify the HindIII and XhoI restriction sites on the cloned gene at the respective ends of the sequence: 5′-ACAAGCTTGGCCACCATG-3′ (HindIII 5′-A^AGCTT-3′) and 5′-GTACT AACTTGGAGCTCG-3′ (XhoI 5′-C^TCGAG-3′). The PCR reaction was carried out with a Multigene Gradient PCR thermal cycler (Labnet International) as follows: 1 cycle of 94 °C for 5 min, 29 cycles of 94 °C for 30 s and 47 °C for 30 s, followed by a final stage of 72 °C for 1 min. The PCR products were purified with the PCR Quick-Spin Product Purification Kit (Intron). In order to increase the PCR product yield of fragments longer than 100 bp, 25 μl of the PCR reaction mixture was mixed with 500 μl of binding buffer (provided with the kit) and 150 μl of isopropanol, prior to application on the purification column. Elution was carried out with 50 μl of DDW after 3 min of incubation at RT. The PCR product was digested with 1.5 μl (10 U/μl) of HindIII (Fermentas, Thermo Scientific) and 1.5 μl (10 U/μl) XhoI (Fermentas) to obtain sticky ends, in a reaction mixture that contained 20 μl, i.e., 4–6 mg, of Plasmid DNA, 3 μl of Buffer Rx10 (Fermentas) and 5.5 μl of DDW, and the mixture was incubated in a dry bath at 37 °C for 1 h. The pIZV5-His expression vector was digested with the same enzymes, in a reaction mixture that contained 20 μl, i.e., 4–6 mg, of Insert DNA, 1.5 μl (10 U/μl) of each enzyme, 3 μl of Buffer Rx10 (Fermentas) and 5.5 μl of DDW, and the mixture was incubated in a dry bath at 37 °C for 1 h. Elution products were tested on agarose gel (1%). The pIZV5-His and the PK/PBAN-R insert were then ligated with a T4 DNA ligase (Promega). Aliquots, each of 100 ng, of double-cut insert and of plasmid were incubated with 2 μl of 10× Ligase buffer and 3 units, i.e., 1 μl, of T4 ligase in a final volume of 20 μl. The reaction proceeded at RT for 3 h. The Kozak sequence motif which had been inserted in the course of cloning [20] was excised, together with that of the receptor, when the gene was transferred into the expression vector.

2.6. Stable transfection in Sf9 cells

Both plasmids, with the PK/PBAN-R genes, *Hep*-PBAN-R and *Spl*-PBAN-R, were stably transfected into *Sf9* with Fugene HD transfection reagent (Roche, Indianapolis, IN, USA). *Sf9* cells (0.5×10^6) were seeded in a 12-well plate (Biofil, Madhya Pradesh, India) overnight. A transfection mixture containing 8 μl of pIZV5-His-PK/PBAN-R (1600 ng of either *Hep*-PK/PBAN-R or *Spl*-PK/PBAN-R), and 3.2 μl of liposomes in DDW at a final volume of 100 μl was incubated at RT for 15 min and then added drop-wise to each well, which contained 1 ml of complete Grace's insect medium. After 72 h the culture medium was replaced with fresh complete Grace's insect medium containing Zeocin (Invitrogen) at 1000 μg/ml, and the cells were grown for 3 weeks in the presence of the antibiotics. The surviving cells (foci) were placed in zeocin-free complete Grace's insect medium and used for further experiments or subjected to re-growth cycles. *Sf9* cells that were stably transfected with an 'empty' pIZ/V5-His vector containing no PK/PBAN-R gene were grown under the same conditions and served as negative controls.

Initial transfection efficiency was determined with a pIZV5-His green fluorescence protein (pIZV5-His-GFP) construct (kindly provided by Dr. A. Zilberstein from the Department of Plant Sciences, George S. Wise Faculty of Life Sciences, Tel Aviv University, Israel) under the same conditions as described above (this section). GFP expression was monitored by observing fluorescence for 24–72 h with a model MZFL111 fluorescence microscope (Leitz, Wetzlar, Germany). The procedure usually yields an initial positive-transfection rate of >90%, as determined by the number of cells transfected with the pIZ/V5-His-GFP plasmid construct.

2.7. Hep and Spl-PK/PBAN-R immunostaining

Sf9 transfected cells (0.5×10^6) were seeded on a round cover glass (Menzel-Glaser, Braunschweig, Germany) in 1 ml of complete Grace's insect medium in a 12-well plate (Biofil) and kept at 27 °C overnight. On the day of the experiment the growth medium was removed and cells were fixed with 0.5 ml of 4% (w/v) paraformaldehyde (Sigma) in phosphate buffered saline (PBS), comprising 0.15 M NaCl and 0.05 M sodium phosphate buffer at pH 7.2, for 15 min. The cells were then washed twice with 0.5 ml of PBS for 10 min. A volume of 0.5 ml of 0.1 M glycine in PBS was added to

each well and after 20 min the cells were washed again for 5 min with 0.5 ml of PBS. An 0.5-ml aliquot of anti-PK/PBAN-R antibodies [21] or pre-immune serum (PI) diluted 1:2500 (*Hep*-PK/PBAN-R) and 1:1250 (*Spl*-PK/PBAN-R) in PBS was added and the mixture was incubated for 1 h at RT and washed for 5 min three times. Blocking was carried out with 0.5 ml of 5% normal goat-serum (NGS) in PBS for 1 h and was followed by three 20-min washing steps. A 0.5-ml aliquot of Alexa goat anti-rabbit conjugate diluted 1:500 in PBS (Molecular Probes, Carlsbad, CA, USA) was added, and the cells were incubated for 1 h at RT after which the incubation wells were washed four times for 1 min with PBS, and 0.5 ml of propidium iodide diluted 1:300 in PBS was added to each well and left for 1 h to stain the nuclei. The wells were washed twice with 0.5 ml PBS for 5 min, the cover glasses were removed from the wells, dried and fixed on a microscope slide with 25 μl of Mowiol mounting medium (polyvinyl alcohol 4–88; Sigma) which was prepared as follows. A 25-g aliquot of Mowiol was mixed with 100 ml of 0.015 M phosphate buffer at pH 8.0 for 16 h at RT, 2 ml of glycerol (MP Biomedics, Solon, OH, USA) were added and mixed for a further 16 h. The mixture was centrifuged at 11,200 ×*g* for 15 min at 4 °C, and the supernatant was removed, aliquoted and stored at −20 °C. The slides were examined with a Fluoview 500 inverted laser scanning confocal microscope, model IX81 (Olympus, Tokyo, Japan). Alexa fluorophore was monitored at an excitation wavelength of 488-nm and an emission wavelength of 519 nm through a BA 505- to 525-nm filter; PI was monitored at an excitation wavelength of 543 nm and an emission was monitored through a BA 610- to 660-nm filter. Images were taken with a 60 × 10 × 2 objective.

2.8. Confocal microscopic examination of calcium influx

Samples, each of 5×10^5 *Hep*-PK/PBAN-R-transfected or *Spl*-PK/PBAN-R-transfected *Sf9* cells, cells transfected with an 'empty' pIZ/V5-His vector, and control *Sf9* cells were seeded in cell microscopy 6-well chambers (1 μ-Slide VI; Ibidi, Martinsried, Germany) with 100 μl of complete Grace's insect medium, and incubated overnight at 27 °C. On the day of the experiment the cells were washed twice with 100 μl of cold PBS, pH 7.2, and 100 μl of 2 μM (final concentration) Fluo-4-AM made up in modified Ringer's buffer (12 mM NaCl, 21 mM KCl, 170 mM glucose, 3 mM $CaCl_2$, 18 mM $MgCl_2$, and 10 mM PIPES, at pH 7.4, containing 1 mM Probenecid and 0.01% Pluronic F-127, all purchased from Sigma, made up in modified Ringer's buffer), were added and they were incubated for 45 min at RT in darkness. They were quickly rinsed twice with 100 μl of cold PBS and kept in darkness for another 30 min to allow hydrolysis of the Fluo-4-AM ester bond. For microscopic observation the buffer was aspirated from the wells and the slides were placed in the confocal microscope and challenged with 80 μl of either modified Ringer's buffer as a negative control, 1 pM PBAN or 1 pM DH made up in modified Ringer's buffer and 1 μM Ionomycin made up in 0.1 M glycine buffer at pH 10.0. Cells were monitored for fluorescence for 10 s prior to peptide addition (baseline determination) and for 60 s after addition of the peptide, buffer or Ionomycin. Fluorescence was monitored at an excitation wavelength of 488 nm, and the emission was monitored through a BA 505- to 525-nm filter. All microscope observations and time-lapse microscopy were performed with an FV500 IX-81 inverted laser scanning confocal microscope (Olympus, Tokyo, Japan) equipped with a 488-nm argon-ion laser and UplanSApo 40× (0.9 N.A.) objective. Thirty time-lapse photos were taken at 3.26-s intervals. Images were taken with a 40× objective. A real-time video of the Ca^{2+} flux into *Hep*-PK/PBAN-R-transfected *Sf9* cells, in response to 1 pM PBAN is presented as supplemental material (Supplemental Video).

2.9. Quantitative analyses of calcium influx

Cells were grown overnight in 25-cm^2 flasks, as described in Section 2.3. On the day of the experiment 4×10^6 cells of each of the following lines were harvested and transferred into 15-ml glass tubes: control untreated *Sf9* cells; cells transfected with an 'empty' pIZ/V5-His vector; *Sf9* cells stably expressing *Hep*-PK/PBAN-R or *Spl*-PK/PBAN-R. Growth medium was removed by centrifugation at 800 ×*g* for 10 min, the pellet was resuspended in 4 ml of PBS at pH 7.2, and centrifuged again under the same conditions. The pellet was then resuspended in 4 ml of modified Ringer's buffer containing 2 μM Fluo-4-AM in DMSO (Molecular Probes, Carlsbad, CA, USA), at a final concentration of 0.25%. Cells were incubated for 45 min on a rotating shaker at a low speed at RT in darkness. After incubation the cells were washed twice with 4 ml of Ringer's modified buffer, followed each time by centrifugation as above (this section), resuspended in 4 ml of Ringer's modified buffer and kept in darkness for another 30 min on a rotating shaker to allow hydrolysis of the Fluo-4-AM ester bond. Cell suspension aliquots of 80 μl, containing 10^5 cells, were placed in each well of a black 96-well plate with a clear bottom (Greiner, Frickenhausen, Germany) and 20 μl of 5× concentrated PBAN or DH made up in Ringer's modified buffer were injected into each well at final concentrations ranging from 1 fM to 10 μM. At the end of the experiment Ionomycin (Alomone Laboratories, Jerusalem, Israel), made up in 0.1 M glycine buffer at pH 10.0, was added to the individual wells at a final concentration of 10 μM in order to determine the maximal positive Ca^{2+} influx response. Each peptide was tested in quadruplicate at each concentration. Fluorescence was measured with a Tristar LB 941 plate reader (Berthold Technologies, Bad Wildbad, Germany) with a 485-nm excitation filter and the signal was monitored via a 535-nm emission filter. Each well was monitored separately. Fluorescence was monitored every second for 5 s prior to addition of the tested peptide or ionomycin to determine the baseline, and every second for 2 min following addition of the peptide or ionomycin. The results are presented as the ratio (expressed as a percentage) between the signal obtained at each peptide concentration and that of ionomycin after subtraction of the background (baseline) value.

2.10. Homology-based modeling of PBAN-R

Three-dimensional homology models of PBAN-R were built for both *Hep*- and *Spl*-PK/PBAN-R sequences. Each amino-acid sequence was aligned with the sequences for all receptors for which structures have been deposited in the protein data base (PDB), to detect homologous proteins available to serve as templates. Alignment was done by using the Hidden Markov Model (HMM) algorithm in the HHpred bioinformatics tool kit [22]. The six structures that scored the highest E values were selected to serve as templates for the corresponding models. The selected structures included representatives of five different GPCR structures. The final alignment of the closest homologous sequences was transferred to Modeler 9.9 [23], in order to obtain initial model coordinates. These steps were further refined by introduction of the putative disulfide bond between C113 and C194, which was followed by short loop refinement with Modeler 9.9. Visualization of the resulting models was obtained by using PyMol [24]. Electrostatic surfaces were calculated with vacuum electrostatic calculation as implemented in PyMol.

2.11. Statistical analysis

All results were subjected to one-way ANOVA. The significant differences among means were evaluated by application of the Tukey–Kramer honestly significant difference (HSD) test at $p < 0.05$. The data are presented as means ± SEM.

3. Results

3.1. Cloning of H. peltigera PBAN-R

In order to isolate the full-length cDNA of the *Hep*-PK/PBAN-R gene, gene-specific PCR primers were designed, based on the

high-homology regions of *H. zea*, *H. armigera*, *B. mori*, *H. virescens* and *S. littoralis* PBAN-R genes [6,7,10,25]. Pheromone gland cDNA was used as a PCR template with the sense and antisense primer pair 5′-ATGACATTGTCAGCGCCC-3′ and 5′-TCACCTTGAAGGCGTTTG-3′, respectively. This successfully amplified a 1200-bp fragment. In order to determine the ORF of the *H. peltigera* gene, gene-specific primers of the 3′ end of *H. zea*, *H. armigera*, *H. virescens* and *S. littoralis* genes were designed and used to amplify the gene, with the 1200-bp fragment used as a template. The only pair of primers that resulted in a PCR product was that of the *H. virescens* C terminal region — sense and antisense 5′-ATGACATTGTCAGCGCCC-3′ and 5′-TCAAACCTTGAAGGCGTTTC-3′, respectively which provided a full-length ORF of 1029 bp. Based on this sequence a 342-amino-acid protein was predicted (Fig. 1). The very first ATG present in the entire cDNA also encoded the initial codon of the putative ORF. Further analysis of the *Hep*-PK/PBAN-R showed that this protein contained several characteristic features of seven TM GPCR (Fig. 2A), including three putative N-linked glycosylation sites – $Asn^{20, 22, 187}$ – that regulate the cell-surface localization and function [26] and an ERY motif – amino acids 137–139 – immediately following the third TM domain, which is a variant of the DRY motif that is responsible for G-protein interaction [27]. Interestingly, the Glu at the C-terminus of TM6, which has also been hypothesized to stabilize the inactive state of some GPCRs, has been replaced by the uncharged amino acid, Gln^{286}. No Ser, Thr or Tyr residues, which serve as potential

```
1    ATGACATTGTCAGCG CCCCCGAGCATCGAC GACTATGAGGAGTCA TTCGAGATGAACACG
                                                         ★
      M  T  L  S  A   P  P  S  I  D   D  Y  E  E  S   F  E  M  N  T
61   ACGAACGTGACGAGT CACCCCGCCGCCTAC GACGAACAGTACGCG CTCGACCTGGTCGTG
        ★
      T  N  V  T  S   H  P  A  A  Y   D  E  Q  Y  A   L  D  L  V  V
121  CCGCTCACCGTCACC TATGTCATCATCTTC GTGGCTGGCATCCTG GGAAACACCAGCACG

      P  L  T  V  T   Y  V  I  I  F   V  A  G  I  L   G  N  T  S  T
181  TGCGTGGTCATAGCC AGGAATCGCTCTATG CACACAGCCACCAAC TTTTACCTCTTCAGT

      C  V  V  I  A   R  N  R  S  M   H  T  A  T  N   F  Y  L  F  S
241  CTAGCAATATCAGAC CTCATATTATTAGTA TGTGGCTTACCCTTT GAGGTACATAGATTA

      L  A  I  S  D   L  I  L  L  V   C  G  L  P  F   E  V  H  R  L
301  TGGAATCCGGACACG TATCCATTAGGCGAG GCGCACTGCATCGCC ATCGGGCTGGCGTCA

      W  N  P  D  T   Y  P  L  G  E   A  H  C  I  A   I  G  L  A  S
361  GAAACGTCAGCCAAC GCGACAGTATTGACA ATAACAGCGTTCACG GTGGAGCGGTACATA

      E  T  S  A  N   A  T  V  L  T   I  T  A  F  T   V [E  R  Y] I
421  GCGATATGTCGACCC TTCATGTCGCACACC ATGTCCAAGCTGTCA AGAGCCGTGCGGTTC

      A  I  C  R  P   F  M  S  H  T   M  S  K  L  S   R  A  V  R  F
481  ATAATAGCTATATGG GTGTTTGCGTTGTGC ACCGCCGTGCCACAA GCGATGCAGTTCGGT

      I  I  A  I  W   V  F  A  L  C   T  A  V  P  Q   A  M  Q  F  G
541  ATAGTGTCGTATGTT GATCATGGGCAGAAT GTGAGCGCGTGTACA GTGAAGGGTGTGGGG
                                 ★
      I  V  S  Y  V   D  H  G  Q  N   V  S  A  C  T   V  K  G  V  G
601  GTCCATCAAGTGTTT GTTATATCTAGTTTC GTGTTCTTCGTGGTG CCTATGTCGATGATA

      V  H  Q  V  F   V  I  S  S  F   V  F  F  V  V   P  M  S  M  I
661  TCAGTGTTGTATGCA TTGATAGGCATTAAG TTGCGGACCTCTCGA GTGTTGCATCCCGTT

      S  V  L  Y  A   L  I  G  I  K   L  R  T  S  R   V  L  H  P  V
721  AAGAAGCTGTCAGTG GAGAGTAATGAGAGA CCTGGACAGATGCAG TACAGGAATGGTGCC

      K  K  L  S  V   E  S  N  E  R   P  G  Q  M  Q   Y  R  N  G  A
781  TCACAAAGAAGAGTC ATCAGAATGCTTGTT GCAGTGGCGCTATCA TTCTTCATTTGCTGG

      S  Q  R  R  V   I  R  M  L  V   A  V  A  L  S   F  F  I  C  W
841  GCGCCTTTCCACGTA CAAAGACTGCTGGCT ATCTACGGGAAAAGC TTGGAGCACCCATCA

      A  P  F  H  V   Q  R  L  L  A   I  Y  G  K  S   L  E  H  P  S
901  GATACCTTCTACCTG GTCTACATCGTACTG ACATTTTTATCGGGG GTGCTATATTTCCTG

      D  T  F  Y  L   V  Y  I  V  L   T  F  L  S  G   V  L  Y  F  L
961  TCGACCGCCATCAAC CCCTTCCTTTACAAC ATTATGTCAAACAAG TTCAGAAACGCCTTC

      S  T  A  I  N   P  F  L  Y  N   I  M  S  N  K   F  R  N  A  F
1021 AAGGTTTGA

      K V  ***
```

Fig. 1. Nucleotide and deduced amino acid sequence of *Hep*-PK/PBAN-R. The nucleotide sequence is numbered from the 5′ to the 3′ direction. Key features of the gene are marked. The TGA stop codon is underlined in bold print. The deduced amino acid sequence of the ORF is shown below the nucleotide sequence for each codon. Potential N-linked glycosylation sites ($Asn^{20, 22, 187}$) are indicated by an ★; the ERY variant of the DRY motif is indicated by boxed letters; GenBank accession no. JN648826.

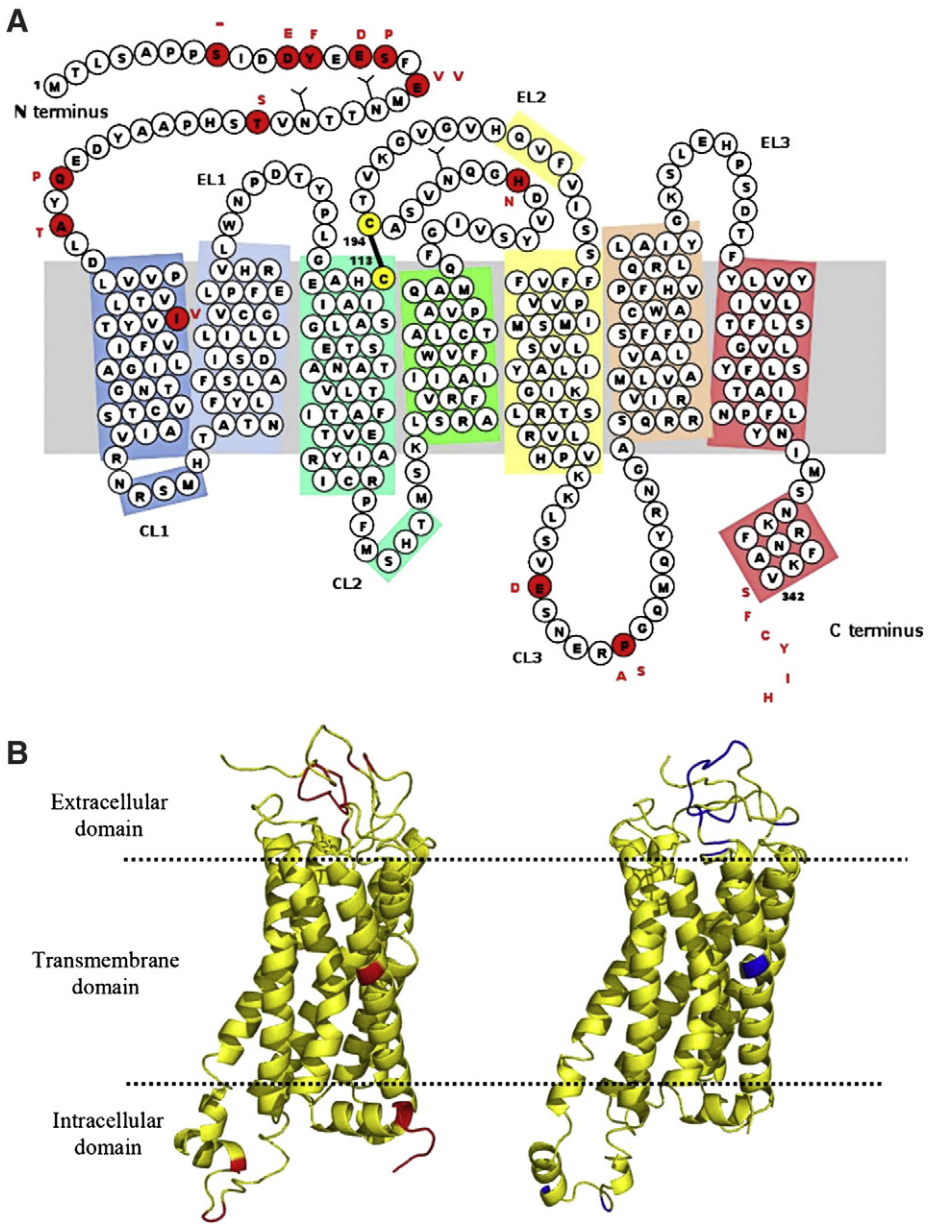

Fig. 2. Homology-based structural models of *Hep*- and *Spl*-PK/PBAN-R. A. A 2-D diagram of *Hep*-PK/PBAN-R sequence in relation to the secondary structural elements. Rainbow-colored boxes represent 7 TM helixes of the GPCR and additional predicted α helices in C-terminus and loops, as obtained in the homology-based model. ECL and ICL loops, as well as N- and C- termini, are emphasized. The putative disulfide bond between C113 (TM helix III) and C194 (EL2) is highlighted in yellow. Putative N-kinked glycosylation sites are represented by stick figures. The amino acids highlighted in red represent the sequential diversity between *Hep*- and *Spl*-PK/PBAN-R. B. Cartoon representation of *Hep*-PK/PBAN-R (right) and the *Spl*-PK/PBAN-R (left) structural models. Models were built as described in the text. Major differences between the primary sequences of the two receptors are highlighted in blue (*H. peltigera*) and red (*S. littoralis*), respectively.

phosphorylation sites, were identified on the C-terminal tail (Fig. 1). The sequence of the *Hep*-PK/PBAN-R has been deposited in the GenBank data base (accession no. JN648826).

3.2. Homology, structural and electrostatic analyses

A BLAST homology analysis of the *Hep*- and the *Spl*-PK/PBAN-Rs based on amino acids demonstrated a rather high similarity with 95% sequence homology, and 98, 98, 97 and 83% homologies with the deduced amino acid sequences of the PK/PBAN-Rs of *H. zea*, *H. armigera*, *H. virescens*, and *B. mori*, respectively. Prediction of the secondary structures of the two receptors by means of the TMHMM Server v. 2.0 indicated the presence of seven TM helixes, three extra-cellular loops (ECLs), three intra-cellular loops (ICLs), a 41-amino-acid long N-terminus, and a rather short C-terminus (Fig. 2A). These characteristics are typical of GPCRs. The three-dimensional structures of *Hep*- and *Spl*-PK/PBAN-Rs were predicted using homology modeling techniques (Fig. 2B). The suggested models were built by using six representative GPCR crystal structures available in the PDB. Although rather low sequence homology has been observed between the two receptors and the structures used for homology modeling (14–17%), the resulting three-dimensional models were clearly shown to fit the predicted secondary structure and, in addition, to show that highly conserved amino acid residues were modeled to the same structural positions [3], as experimentally shown for class A GPCRs. Both structures contained two conserved Cys residues modeled to the extracellular domains: Cys^{113} which is located in TM helix III; and Cys^{194}, located in the second ECL. In

light of the fact that these residues are known to form a disulfide bond, a putative disulfide bond has been built into both structural models (Fig. 2A). The resulting models were shown to be significantly different at their N-termini. Additional differences were apparent in the positions of the second ECL, the third ICL, and the C-terminus. Also, a smaller difference was observed at position 48, where an Ile residue present in *H. peltigera* was replaced with Val in *S. littoralis* (Fig. 2A). A comparison between the electrostatic potentials calculated for the two receptor models revealed a large net charge difference in the extracellular regions and a smaller one at the C-terminus region of the protein (Fig. 3). Since these two domains are proposed to perform peptide-binding and signal transmission, respectively, the prediction that these putative differences can lead to differential receptor-ligand interactions and peptide functionalities.

3.3. Stable expression of the H. peltigera and the S. littoralis PBAN-Rs in Sf9 cells

In order to determine the cellular functionality of the receptors and to find out whether the structural and electrostatic differences affect the ability of the receptor to bind different PK/PBAN ligands, both receptors were stably expressed in *Sf9* cells, and their ability to respond to different peptides was monitored with Ca flux experiments. The vector that was chosen for stable transfection of *Sf9* cells was pIZ/V5-His, derived from the multicapsid nuclear polyhedrosis baculovirus which contains a Zeocin antibiotic-resistance gene for selection of stably transformed cell lines. In order to be able to insert the *Hep*-PK/PBAN-R gene into the pIZ/V5-His vector two restriction sites – BamHI and XbaI – were constructed, along with a Kozak sequence to enhance the expression of the gene in the cells. The *Spl*-PK/PBAN-R gene was originally inserted into a pCR2.1 cloning vector [20]. In order to insert it into the pIZ/V5-His expression vector the gene was excised from the pCR2.1 vector, subjected to a PCR reaction with specific primers that were designed to add a HindIII enzyme restriction site and a Kozak sequence prior to the gene start codon-ATG, and a XhoI enzyme restriction site after the stop codon.

The pIZ/V5-His vector, with either the *Hep*- or the *Spl*-PK/PBAN-R gene, was transfected into *Sf9* cells by means of Fugene HD transfection reagent and selection of successfully transfected cells was carried out with zeocin for 3 weeks. Surviving cells were cultured to increase numbers, analyzed for PK/PBAN-R expression and used to analyze the Ca flux elicited by PK/PBAN peptide ligands. Successful expression was confirmed by means of a fluorescent immuno-cytochemical (ICC) staining method that used anti-PK/PBAN-R antiserum to visualize the *Spl*- and *Hep*-PK/PBAN-R. The results revealed (Fig. 4A and C) that the receptors were localized exclusively to the plasma membrane of the transfected cells. Expression of the receptor was obtained only in *Sf9* cells transfected with pIZ/V5-His PK/PBAN-Rs stained with the anti-PK/PBAN-R antiserum (Fig. 4A and C); no staining was obtained when the cells were treated with pre-immune serum (Fig. 4B and D). Control cells, transfected with the pIZ/V5-His vector that did not contain the PK/PBAN-R insert, that underwent the same treatments, did not show any green fluorescence signal, either on the cell membrane or in the cytoplasm (Fig. 4E and F, respectively).

3.4. Confocal-microscopy-based Ca imaging

Next, we determined whether the structural and electrostatic differences between N- and C-terminal parts of the *Hep* and *Spl*-PK/PBAN receptors affect binding of different PK/PBAN ligands. This was determined by monitoring Ca flux upon stimulation of both receptors with different ligands. Two ligands of the PK/PBAN family were chosen for the analysis: PBAN and DH. *Sf9* cells transfected with *Hep*- or *Spl*-PK/PBAN-R were incubated with Fluo-4 AM, rinsed, placed in the confocal microscope and challenged with 1 pM PBAN or DH, or 10 μM ionomycin. Baseline fluorescence was monitored for 10 s prior to peptide or ionomycin addition. Untransfected *Sf9* cells and cells transfected with an 'empty' pIZ-V5/His vector served as control cells. The data in Fig. 5 and in Supplemental Video clearly reveal very high responses of *Hep*- and *Spl*-PK/PBAN-R to 1 pM PBAN, indicating that both receptors were fully functional in the stably transfected cell line. The response to the same concentration of DH differed between the two cloned receptors: DH stimulated Ca flux in *Spl*-PK/PBAN-R-transfected cells, whereas no response was detected in the *Hep*-PK/PBAN-R. Untransfected *Sf9* cells stimulated with the peptides at the same concentration did not exhibit Ca flux (Fig. 5), and the same results were obtained with treated cells transfected with an 'empty' pIZ-V5/His vector (data not shown). Ionomycin stimulated Ca flux in all three cell lines (Fig. 5).

3.5. Functional characterization of stably expressed Hep- and Spl-PK/PBAN-Rs

In order to further evaluate the cellular functional differences between the two receptors dose-response experiments were carried out in which Ca flux was monitored in cells expressing *Hep*- or *Spl*-PK/*PBAN-Rs* that were stimulated by various concentrations of either PBAN or DH. The results revealed different responses to both peptides at different concentrations. At low concentrations, up to 100 pM, both receptors showed very high sensitivity to PBAN, with responses in the fM–pM range. In the presence of the peptide both receptors showed

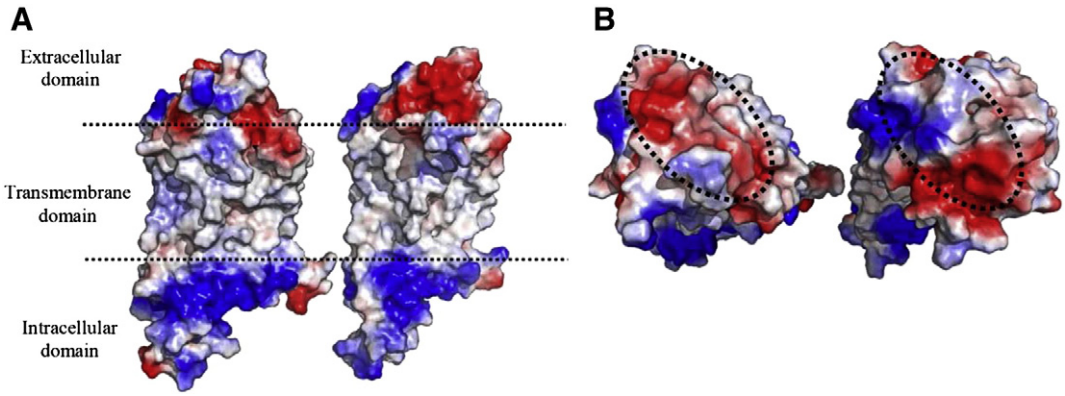

Fig. 3. Visualization of calculated surface electrostatic potentials of *Hep*- and *Spl*-PK/PBAN-R models. A. Surface representations of *Hep*-PK/PBAN-R (right) and *Spl*-PK/PBAN-R (left) models, colored according to their calculated vacuum electrostatic potentials, indicating a net positive charge (blue) in the intracellular regions of both receptors, and a net negative charge in the extracellular loops (red). B. A view of the extracellular domain region from above the plane of the membrane of the two receptor models, illustrating the differences of electrostatic potential in the ligand's binding vicinity. Most differences result from high variance in the N-terminal region.

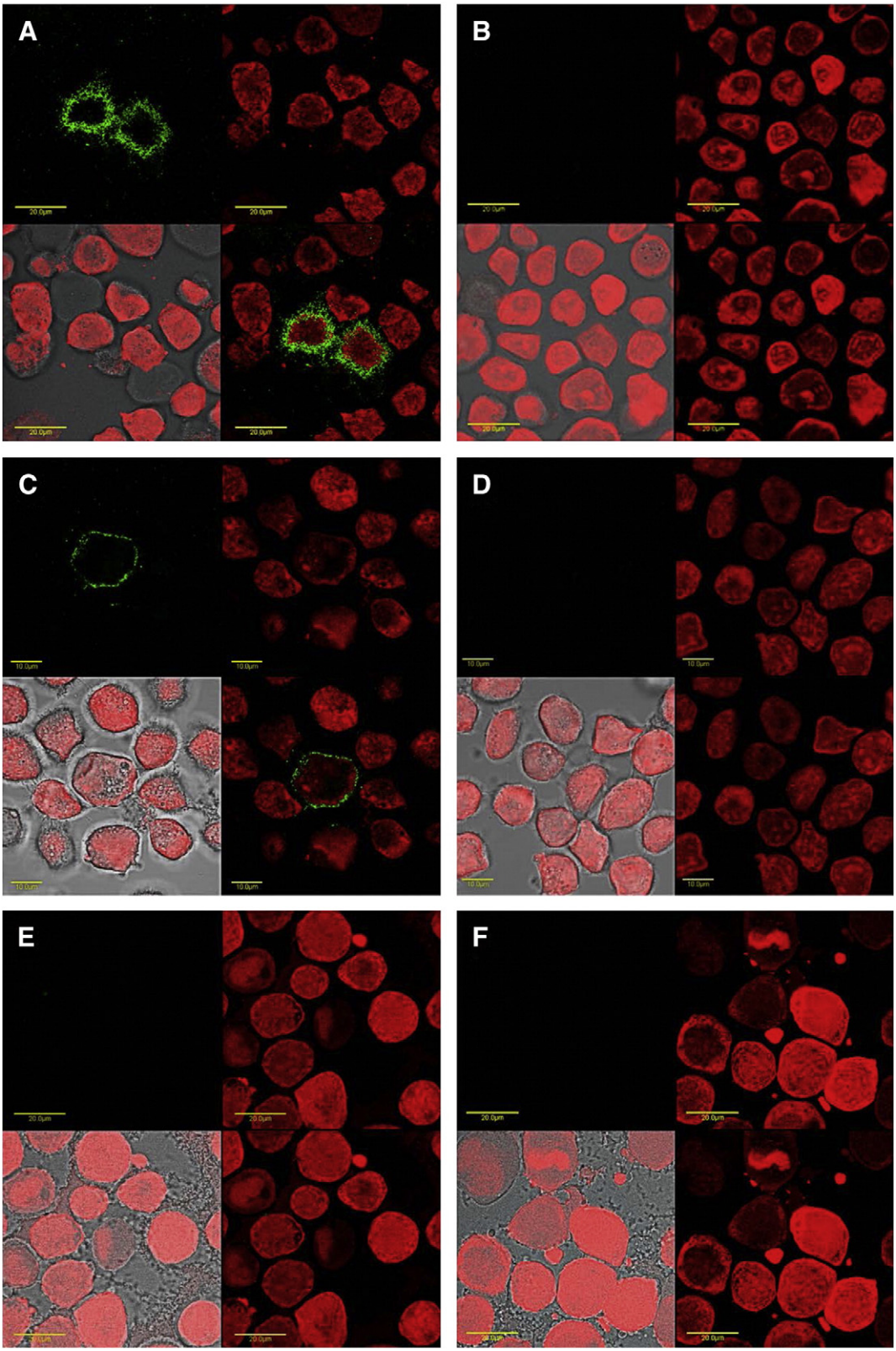

Fig. 4. Immunostaining of *Hep*- and *Spl*-PK/PBAN-R stably expressed in *Sf9* cells. *Spl*-PK/PBAN-R-transfected cells stained with anti-PK/PBAN-R antiserum (A); *Spl*-PK/PBAN-R-transfected cells stained with PI serum (B); *Hep*-PK/PBAN-R-transfected cells stained with anti-PK/PBAN-R antiserum (C); *Hep*-PK/PBAN-R-transfected cells stained with PI serum (D); cells transfected with pIZV5-His 'empty' vector stained with anti-PK/PBAN-R antiserum (E) or PI serum (F). Primary Ab binding is indicated by green color. Cell nuclei were stained with propidium iodide (red color). Bar represents 20 μM (panels A, B, E and F) or 10 μM (panels C and D). Each image represents data obtained in three independent experiments. Panels represent (clockwise from upper left): alexa, propidium iodide; superposition of Alexa on propidium iodide staining; superposition of phase over propidium iodide.

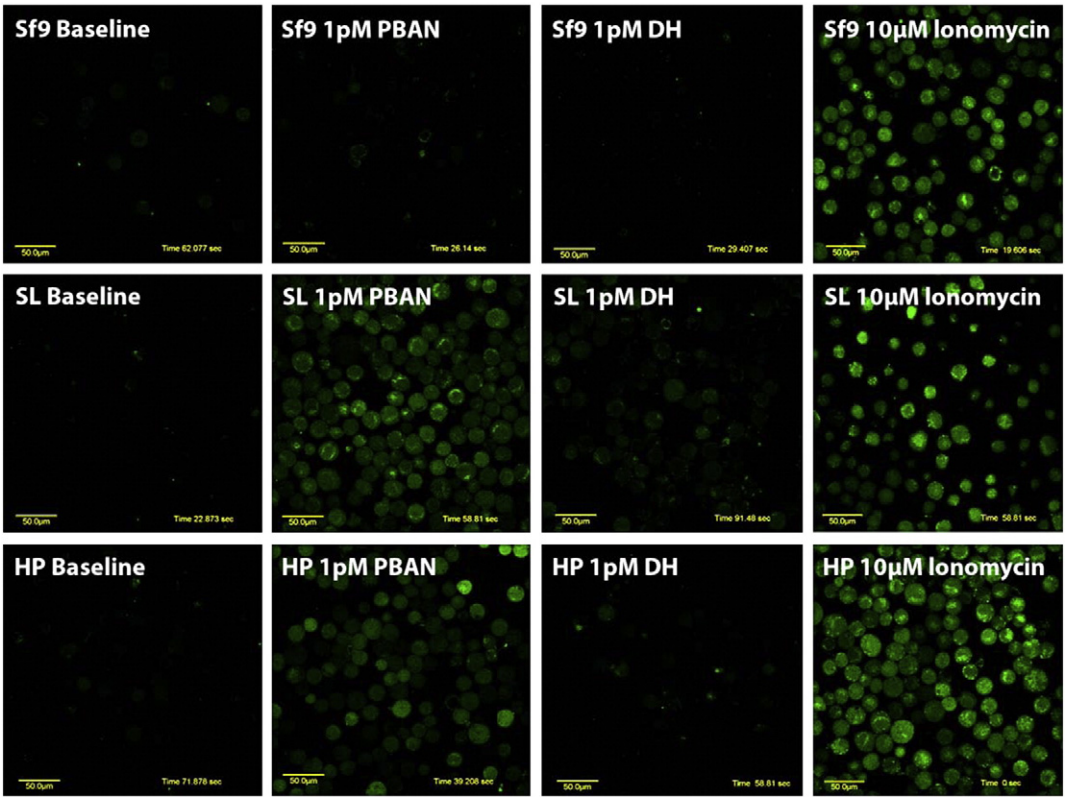

Fig. 5. Confocal microscope images of functional expression of *Hep*-PK/PBAN-R (HP) and *Spl*-PK/PBAN-R (SL) in stably transfected *Sf9* cells. Cells were incubated with the Ca^{2+} indicator (baseline) and then challenged with PBAN, DH or ionomycin. Bar represents 50 μM. Each image represents data obtained in three independent experiments.

gradual increases in Ca flux in the PBAN concentration ranges of 0.001–10 pM, with EC_{50} values of 0.15 and 0.12 pM, for *Hep*- and *Spl*-PK/PBAN-R, respectively (Fig. 6A and B). Higher PBAN concentrations, up to 10 μM revealed differences between both receptors. A bi-phasic response was obtained with the *Hep*-PK/PABN-R, with a peak of activity at 10 pM and a second peak of activity at 100 nM. No response was obtained with the *Spl*-PK/PBAN-R at PBAN doses higher than 100 pM (Fig. 6A and B). The responses of the two receptors to DH also differed significantly: DH at the fM–pM range elicited a high flux of Ca in the *Spl*-PK/PBAN-R, with EC_{50} of 0.013 pM, whereas, in the same concentration range it did not elicit Ca flux in the *Hep*-PK/PBAN-R, and the fluorescence signal did not differ significantly from that elicited by the buffer (Fig. 7A and B). The maximal response of the *Spl*-PK/PBAN-Rs to DH and the EC_{50} value were an order of magnitude lower than those to PBAN (0.013 vs. 0.12 pM, respectively). Also, the range of DH activity was broader than that of PBAN: 0.001–1 pM compared with 1–10 pM, respectively. An attempt to elicit a response with DH at concentrations above 10 pM failed to stimulate either receptor (Fig. 7A and B). No stimulation was obtained in the absence of a peptide ligand in any of the experiments, and no response was obtained in *Sf9* cells that were transfected just with a pIZ/V5-His vector that did not contain a PK/PBAN-R gene insert (data not shown).

4. Discussion

In the present study we set out to determine whether different bioactivities elicited by PK/PBAN peptides are mediated by different PK/PBAN receptors, and whether they respond differently to PK/PBAN ligands. The study focused specifically on two receptors: one that mediates sex pheromone production in the pheromone gland of adult female moths, and a second that mediates cuticular melanization in larvae (for review see [1]). To that end, two receptors of the PK/PBAN family – a sex pheromone gland receptor from *H. peltigera* and a *S. littoralis* larval receptor that mediates cuticular melanization – were cloned, stably expressed in *Sf9* cells, and their structural models, electrostatic potentials, and cellular functional properties, as affected by stimulation with different ligands were evaluated. Homology modeling techniques indicated that highly conserved amino-acid residues were modeled to appropriate structural positions, as experimentally shown for class A GPCRs. Despite the high amino-acid homology of 95% between the two receptors, significant structural differences could be predicted to occur at their N-termini, in the second ECL, the third ICL, and the C-terminus. A comparison between the electrostatic potentials calculated for the two receptor models revealed a large net charge difference in the extracellular regions and a smaller one at the C-terminus. Immuno-staining revealed that the PK/PBAN-R gene encoded a cell surface receptor, and calcium-mobilization assays demonstrated that both receptors were fully functional and capable of initiating the first phase of the PK/PBAN signal transduction cascade, i.e., influx of extracellular calcium. Evaluation of the signaling responses of both receptors to PBAN and DH revealed very sensitive, though differential responses to the two peptides.

When modeling members of the very large GPCR family, it is quite apparent that the most conserved trans-membrane regions will be modeled in a rather similar fashion. As the number of crystal structures of GPCRs increases, the potential for variation will increase as well, hopefully leading to the illumination of differences in all of the protein's domains. In the present study, the two receptors were not only derived from two different species, but each represents GPCRs present at two different developmental stages in moth's life cycle and mediates two different bioactivities. Therefore, while there is only about 5% variance in the primary protein sequence, structural attributes, either static or dynamic, should exist that will mediate the different bioactivities exhibited at different stages of a moth's life cycle. Exhibiting the minor sequence differences on the scaffold of the homology based model hint at the possibility that the non-similar areas might result in

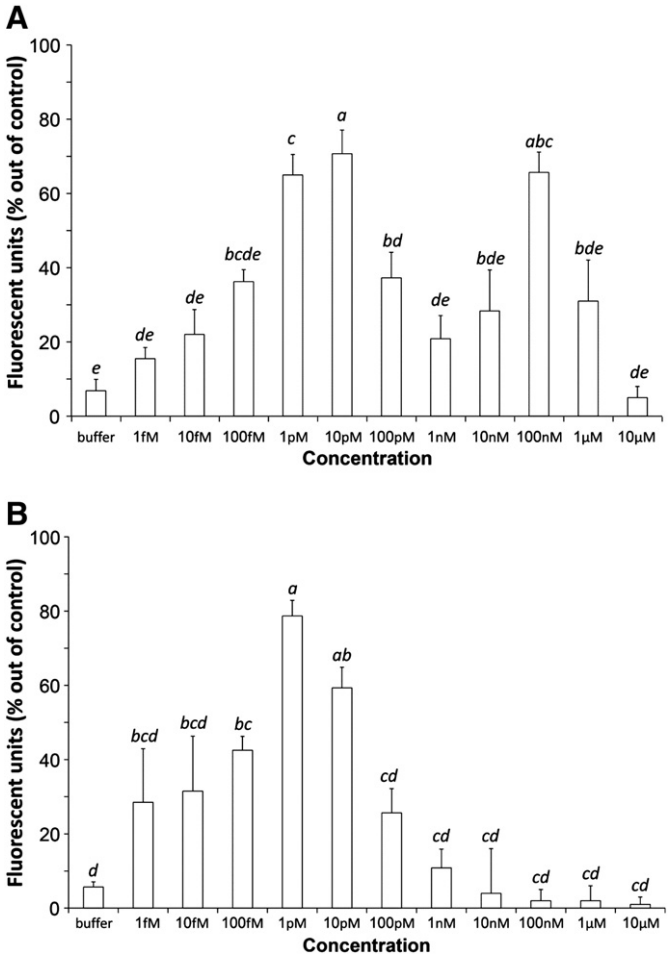

Fig. 6. PBAN-stimulated intracellular Ca^{2+} level in *Hep*-PK/PBAN-R (A) and *Spl*-PK/PBAN-R (B)-expressing *Sf9* cells. The Ca^{2+} response in the absence of PBAN ligand (buffer) was negligible. Results represent the means ± SEM of six or seven independent experiments (*Hep*-PK/PBAN-R and *Spl*-PK/PBAN-R, respectively), each of which included four replicates. The results are presented as the ratio (expressed as a percentage) between the signal obtained at each peptide concentration and that of ionomycin after subtraction of the background (baseline) value. Bars with the same letter do not differ significantly at $p < 0.05$.

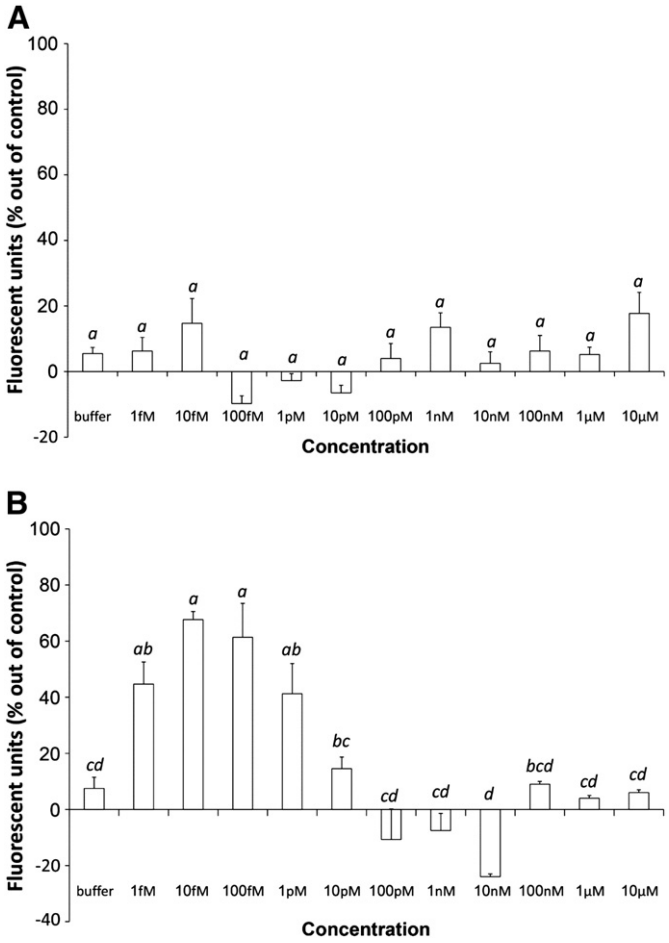

Fig. 7. DH-stimulated intracellular Ca^{2+} level in *Hep*-PK/PBAN-R (A) and *Spl*-PK/PBAN-R (B)-expressing *Sf9* cells. All experimental details are as described in Fig. 6. Results represent the mean ± SEM of four independent experiments each of which included four replicates.

differences in binding and activation and add important information on the structure/activity relationship of such receptors. Similar models were previously used to explore other PK/PBAN receptors from relatively close moth's species [3,28,29], and indeed were shown to clearly fit the predicted secondary structure and in addition, show that some highly conserved amino acids residues are modeled to appropriate structural positions as experimentally shown for class A GPCRs (these elements are thoroughly highlighted at a recent review paper by Jurenka and Nusawardani [3]). The most prominent difference between the two receptors studied here is indeed in these domains, especially at the N-termini, in the second ECL, the third ICL and the C-terminus. A comparison between the electrostatic potentials calculated for the two receptor models revealed a large net charge difference in the extracellular regions (Fig. 3). Since electrostatics is clearly the most important long-range force of attraction, these differences in the regions known to be important for the identification and interaction with ligands might explain the different affinities obtained for the ligands tested in this study toward the two receptors. Our model, showing significant differences in the ECLs is also consistent with nuclear magnetic resonance (NMR) binding assays performed on isolated partial GPCR extracellular domain with different CCK-8 type ligands [30]. This study was able to identify specific residue interactions that differentiate between different receptors. According to this study, binding differentiation is located at both the N-terminal of the GPCR and the N-terminal of peptide ligands. In the two receptors presented here, major differences are indeed found in both the N-termini of the receptors and the ligands, leading to differential binding. The differences observed in the intracellular region might imply that different interaction patterns with G proteins exist downstream in the signal transduction pathway, thus implying for a different receptor cellular functionality. This issue is currently under further investigation.

Until now PK/PBAN-Rs have been cloned from the pheromone gland of seven lepidopteran species three of which are *Helicoverpa* and *Heliothis* species: *H. zea*, *H. armigera* and *H. virescens* [1,8]. Only three of these PK/PBAN-Rs (*Hez*-, *Hev*- and *Bom*-PK/PBAN-R were expressed in cell lines — *Sf9* or Chinese hamster ovary, CHO), and their ability to bind and respond to different ligands originating from the *pban*-gene was tested by observing the resulting Ca^{+2} flux [6,7,10,31,32]. Stimulation of the receptors by *pban*-gene-derived peptides (PBAN, DH, β- and γ-SGNPs) resulted in EC_{50} values in the nM range, i.e., 1.4 and 25 nM PBAN for *Hev*- and *Hez*-PK/PBAN-R, respectively, and an activity range between 1 nM and 1 μM for *Bom*-R. The responses of these receptors to the other peptides, including DH, were similar to those obtained with PBAN. Our present results with the pheromone gland *Hep*-PK/PBAN-R revealed a 4 to 5 orders of magnitude higher sensitivity toward PBAN (EC_{50} of 0.15 pM) and no response over a very wide range of concentration (1 fM–10 μM) toward DH. The reason for the differences in the EC_{50} between our data and those reported in other studies is not fully understood, especially those between the *H. zea*-R and our cloned *H. peltigera* receptor

as *H. zea* and *H. peltigera* are closely related moths and both receptors have been expressed in the same cell line. One possible explanation is that there are different PK/PBAN receptor variants in the pheromone gland and each cloned receptor represents a different variant (as has recently been reported by Lee et al. [8]). It also could be that the differences between the responses of the pheromone gland receptors – associated with the same in vivo functional properties – resulted from use of differing experimental paradigms for their characterization: e.g., different expression systems (stable or transient); use of different cell lines (insect *Sf9* or CHO); use of modified receptors (native or enhanced green fluorescent protein (EGFP)-linked); use of modified ligands (i.e., Rhodamine-labeled PBAN); differing Ca flux indicators; differing equipment sensitivity, etc. [6,7,10,32]. Whatever the reason is the physiological significance of the present data calls for further exploration.

As opposed to the well studied sex pheromone PK/PBAN-Rs to date, only three other larval receptors have been cloned and characterized: two from *H. virescens* moth larvae (variants A and B), which were functionally inactive [10], and one from *D. melanogaster* [33], which responded to β-SGNP and CAPA-DH at 400 and 50 nM, respectively, in contrast to the sub-pM response – EC_{50} of 0.013 pM – of our *Spl*-PK/PBAN-R. The major difference between the responses may result from the nature of the receptors present in evolutionarily distant insect species or, as indicated above, from the differing experimental setups. Support for the possible effect of the experimental setup on the receptors' characteristics comes from our previous study, in which the cloned *Spl*-PK/PBAN-R was stably expressed in NIH3T3 cells and its ability to elicit Ca flux was monitored in the presence of PBAN [20]. Although the receptor responded to PBAN the range of activity was much higher, at 0.1–1 μM, than the sub-pM concentrations obtained in the present study with an *Sf9* insect expression system. Indeed, several previous studies have indicated that the proper receptor ligand interaction is very much dependent upon the choice of the expression system and the mode of expression. For that reason we chose to use the same expression system and experimental paradigm for both our cloned receptors in order to compare the pheromone gland and larval PK/PBAN-Rs. Furthermore, we chose to use an insect cell line – *Sf9* – rather than a mammalian one because, in our opinion, the former is more suitable for expressing and studying insect receptors.

Comparison of the cellular functional properties of the *Hep*- and *Slp*-PK/PBAN-Rs revealed differential responses to both PBAN and DH. Both receptors responded to PBAN with EC_{50} values in the sub-pM range (0.15 and 0.12 pM, for *Hep*- and *Spl*-PK/PBAN-R, respectively), whereas their responses to DH differed significantly. The *Spl*-PK/PBAN-R exhibited a high response to DH, with EC_{50} of 0.013 pM, whereas the *Hep*-PK/PBAN-R was not activated by this peptide over a very wide concentration range — fM to μM. Both receptors did not respond to DH at high concentrations ranging from 100 pM to 10 μM. The receptors also differed in their response at high PBAN concentrations of PBAN; the peptide elicited a biphasic response in the *Hep*-PK/PBAN-R but not in the *Spl*-PK/PBAN-R. The nature of the biphasic response to PBAN is not clear at the moment. The physiological meaning of the biphasic response has to be further evaluated by monitoring differences in secondary messenger pathways (at pM and nM concentrations). Such experiments are currently in progress. Once completed, we may be able to better understand the differences associated with the low and high dose effects of PBAN on the *Hep*-PK/PBAN-R.

In light of these results it is reasonable to assume that sex pheromone biosynthesis is mediated by PBAN whereas larval cuticular melanization is mediated by both PBAN and DH. With this respect it is interesting to note that the differential response of the receptors to PBAN and DH ligands – which share the C-terminal sequence FXPRLa – indicates that the consensus sequence of the family, although important for bioactivity and cross-reactivity of the PK/PBAN peptides, is not the only sequence that determines and contributes to ligand/receptor interactions and there are, most likely, additional residues that play a role in ligand binding. Further studies on this issue are in progress.

To the best of our knowledge this is the first indication, based on a cellular functional response of the actual receptor, of a correlation between a given peptide (or peptides) with a specific bioactivity (sex pheromone production and cuticular melanization) and a direct demonstration of cellular functional differences between both receptors. An indication of possible differences between these two receptors came from our previous studies with conformationally constrained backbone cyclic (BBC) PK/PBAN analogs. BBC compounds exhibit receptor selectivity that results from restriction of the conformational space that, in turn, causes the peptides to mediate one function and exclude it from other functions [14]. Examination of the agonistic and antagonistic properties of the BBC PK/PBAN analogs in in vivo pheromonotropic and melanotropic assays, revealed presence of selective agonists and antagonists toward each function which resulted from differences in the receptors that mediate those functions and, most likely, affected their binding properties [15].

Examination of the responses of other cloned and expressed PK/PBAN-Rs from various insect species, with a variety of ligands, carried out by other research groups, revealed several other receptors that showed a selective response, as indicated by their ability to induce Ca flux. A pupal receptor from *B. mori* responded selectively to *pban*-gene-derived peptides: it exhibited a high response only to *Bom*-DH but not to any of three other peptides — PBAN, β-SGNP and γ-SGNP [34]. Two *D. melanogaster* receptors – *Drm*-CG8784 and *Drm*-CG8795 – selectively responded to *Drm*-β-SGNP but not to *Drm*-DH [35]; and an *Ang*-R of the mosquito *A. gambiae* (termed *Ang*-PK-1) responded to *Ang*-DH but not to *Ang*-PBAN or *Ang*-β-SGNP [36]. In all the above cases the receptor either did not respond to a given peptide ligand or elicited Ca flux at concentrations 3–4 times higher than those required of the active peptides; however no correlation was made between a given peptide (or peptides) with a specific bioactivity.

The differential responses to PBAN and DH raise a few interesting questions with regard to the mode of action of this family of peptides. Molecular cloning of the PK/PBAN peptides revealed that PBAN is encoded by the *pban*-gene, which also encodes DH, as well as other peptides. A peptide that contains the consensus sequence – WFGPRLa – typical of DH (WFGPRLa) is also encoded by the *capa*-gene and is termed CAPA-DH. This raises the question of whether the selective response of the two receptors indicates responsiveness of the *Spl*-PK/PBAN-R to both gene products – *pban*-gene-derived PBAN and DH and *capa*-gene-derived DH – and that of the *Hep*-PK/PBAN-R only to the *pban*-gene product — PBAN. This issue will be resolved once the *capa*-gene-derived DH amino acid sequences from *S. littoralis* and *H. peltigera* will be sequenced.

Another interesting issue with this respect relates to the fact that PBAN and DH are contained within the same prohormone encoded by the *pban*-gene. Thus, unless there are special cell-type differential processing mechanisms, such as those found for the *capa*-gene in *D. melanogaster* and *B. mori* [37,38], both peptides must be produced and released in equimolar amounts by the neurosecretory cells. Thus, the inability of the DH to stimulate the *Hep*-PK/PBAN-R pheromone gland receptor seems peculiar, especially in light of the fact that DH elicits sex pheromone biosynthesis in vivo in *H. peltigera* females — albeit at a 10-times higher dose than PBAN (Altstein et al., in preparation). This raises the possibility that DH may act on another receptor present in the pheromone gland. Indeed, recent studies have shown concurrent expression of multiple PK/PBAN pheromone gland receptor variants that arise from alternative splicing of the 3′ coding region in several moth species (*B. mori*, *H. zea*, *H. armigera* and *P. separata*) — variants that share a significant homology and differ from each other in an extended C-terminal sequence. Attempts to clone such receptors from the *H. peltigera* and *S. littoralis* moths are needed, in order to check whether there are additional variants in these two insects

and to characterize their cellular functional properties in response to stimulation with different PK/PBAN ligands. The possible presence of two or more receptors for a single gene product suggests that several simultaneous physiological processes have to be coordinated or synchronized in order to elicit a given biological activity. Studies along these lines should be further explored.

In summary: many attempts have been made to characterize the PK/PBAN receptors, in efforts to gain a better insight into the mode of action of this family of Nps and into the molecular mechanisms underlying the wide variety of functions mediated by them. The present findings presented in this study, on the structural and cellular functional differences between the two receptors form strong and direct evidence for the notion that different PK/PBAN in vivo functions are mediated by different PK/PBAN receptors, and they hint at the possibility that each function might be elicited by a different peptide or peptides. With this respect it is interesting to note that, despite the high homology – 95% based on amino-acid BLAST – between the *Hep*- and the *Spl*-PK/PBAN-Rs they differed markedly in their three-dimensional structures, electrostatic potentials, and ligand binding properties, indicating that classification of receptors into families on the basis of sequence homology alone does not provide sufficient information on their physiological and pharmacological properties. Cloning and stable expression in cell lines of the PK/PBAN-Rs may now pave the way to answering some of the key questions regarding the bioactivity of this family of Nps. Further research with these expressed receptors will aim to identify additional conformation aspects that are critical to the binding of *pban*- and *capa*-gene-derived peptides to the active site, and their activation, and also to explore the respective signaling pathways associated with the activation of the various receptors by different PK/PBAN ligands. Further characterization of these receptors and of their interactions with the various members of the PK/PBAN family peptides might advance our understanding of their multifunctional nature in moths and other insects, shed light on as yet unknown important processes mediated by the family and help in exploring novel high-affinity receptor-specific antagonists that might serve as a basis for the development of new families of insect-control agents.

Supplementary data to this article can be found online at http://dx.doi.org/10.1016/j.bbagen.2013.06.041.

Acknowledgements

This research was supported by the US–Israel Binational Agricultural Research and Development Fund (BARD) (IS-4205-09) (MA). There is no conflict of interest in publishing the paper. This manuscript forms part of the Ph.D. thesis of Aliza Hariton-Shalev, a student at the Hebrew University of Jerusalem. This paper is contribution no. 507/12 from the Agricultural Research Organization, the Volcani Center, PO Box 6, Bet Dagan 50250, Israel.

References

[1] M. Altstein, A. Hariton, R. Nachman, FXPRLamide (pyrokinin/PBAN) family, in: A. Kastin (Ed.), Handbook of Biologically Active Peptides, Academic Press, 2013, pp. 255–266, (Chapter 37).
[2] Y. Fan, R.M. Pereira, E. Kilic, G. Casella, N.O. Keyhani, Pyrokinin beta-neuropeptide affects necrophoretic behavior in fire ants (*S. invicta*), and expression of beta-NP in a mycoinsecticide increases its virulence, PLoS One 7 (2012) e26924, (1–7).
[3] R. Jurenka, T. Nusawardani, The pyrokinin/pheromone biosynthesis-activating neuropeptide (PBAN) family of peptides and their receptors in Insecta: evolutionary trace indicates potential receptor ligand-binding domains, Insect Mol. Biol. 20 (2011) 323–334.
[4] M. Altstein, O. Ben-Aziz, K. Bhargava, Q.J. Li, M. Martins-Green, Histochemical localization of the PBAN receptor in the pheromone gland of *Heliothis peltigera*, Peptides 24 (2003) 1335–1347.
[5] R.S. Hewes, P.H. Taghert, Neuropeptides and neuropeptide receptors in the *Drosophila melanogaster* genome, Genome Res. 11 (2001) 1126–1142.
[6] M.Y. Choi, E.J. Fuerst, A. Rafaeli, R. Jurenka, Identification of a G protein-coupled receptor for pheromone biosynthesis activating neuropeptide from pheromone glands of the moth *Helicoverpa zea*, Proc. Natl. Acad. Sci. U. S. A. 100 (2003) 9721–9726.
[7] J.J. Hull, A. Ohnishi, K. Moto, Y. Kawasaki, R. Kurata, M.G. Suzuki, S. Matsumoto, Cloning and characterization of the pheromone biosynthesis activating neuropeptide receptor from the silkmoth, *Bombyx mori* — significance of the carboxyl terminus in receptor internalization, J. Biol. Chem. 279 (2004) 51500–51507.
[8] J.M. Lee, J.J. Hull, T. Kawai, C. Goto, M. Kurihara, M. Tanokura, K. Nagata, H. Nagasawa, S. Matsumoto, Re-evaluation of the PBAN receptor molecule: characterization of PBANR variants expressed in the pheromone glands of moths, Front. Endocrinol. (Lausanne) 3 (2012) 1–12, (Article 6).
[9] R. Bober, A. Rafaeli, Gene-silencing reveals the functional significance of pheromone biosynthesis activating neuropeptide receptor (PBAN-R) in a male moth, Proc. Natl. Acad. Sci. U. S. A. 107 (2010) 16858–16862.
[10] Y.J. Kim, R.J. Nachman, K. Aimanova, S. Gill, M.E. Adams, The pheromone biosynthesis activating neuropeptide (PBAN) receptor of *Heliothis virescens*: identification, functional expression, and structure–activity relationships of ligand analogs, Peptides 29 (2008) 268–275.
[11] A.K. Raina, G. Gade, Insect peptide nomenclature, Insect Biochem. 18 (1988) 785–787.
[12] S. Matsumoto, A. Ohnishi, J.M. Lee, J.J. Hull, Unraveling the pheromone biosynthesis activating neuropeptide (PBAN) signal transduction cascade that regulates sex pheromone production in moths, Vitam. Horm. 83 (2010) 425–445.
[13] R. Jurenka, A. Rafaeli, Regulatory role of PBAN in sex pheromone biosynthesis of heliothine moths, Front. Endocrinol. 2 (2011) 1–8.
[14] M. Altstein, O. Ben-Aziz, S. Daniel, I. Schefler, I. Zeltser, C. Gilon, Backbone cyclic peptide antagonists, derived from the insect pheromone biosynthesis activating neuropeptide, inhibit sex pheromone biosynthesis in moths, J. Biol. Chem. 274 (1999) 17573–17579.
[15] M. Altstein, O. Ben-Aziz, I. Zeltser, K. Bhargava, M. Davidovitch, A. Strey, N. Pryor, R.J. Nachman, Inhibition of PK/PBAN-mediated functions in insects: discovery of selective and non-selective inhibitors, Peptides 28 (2007) 574–584.
[16] I. Zeltser, C. Gilon, O. Ben-Aziz, I. Schefler, M. Altstein, Discovery of a linear lead antagonist to the insect pheromone biosynthesis activating neuropeptide (PBAN), Peptides 21 (2000) 1457–1465.
[17] E. Dunkelblum, H. Mamane, M. Altstein, Z. Goldschmidt, Acetylation of alcohols in the pheromone biosynthesis of the tomato looper, *Chrysodeixis chalcites* (Lepidoptera, Noctuidae), Insect Biochem. 19 (1989) 523–526.
[18] G.E. Smith, G. Ju, B.L. Ericson, J. Moschera, H.W. Lahm, R. Chizzonite, M.D. Summers, Modification and secretion of human interleukin 2 produced in insect cells by a baculovirus expression vector, Proc. Natl. Acad. Sci. U. S. A. 82 (1985) 8404–8408.
[19] M. Kozak, Point mutations define a sequence flanking the AUG initiator codon that modulates translation by eukaryotic ribosomes, Cell 44 (1986) 283–292.
[20] L. Zheng, C. Lytle, C.-N. Njauw, M. Altstein, M. Martins-Green, Cloning and characterization of the pheromone biosynthesis activating neuropeptide receptor gene in *Spodoptera littoralis* larvae, Gene 393 (2007) 20–30.
[21] T. Ben Yosef, A. Bronshtein, O. Ben Aziz, M. Davidovitch, I. Tirosh, M. Altstein, PBAN receptor: employment of anti-receptor antibodies for its characterization and for development of a microplate binding assay, J. Insect Physiol. 55 (2009) 825–833.
[22] J. Soding, Protein homology detection by HMM-HMM comparison, Bioinformatics 21 (2005) 951–960.
[23] A. Sali, T.L. Blundell, Comparative protein modelling by satisfaction of spatial restraints, J. Mol. Biol. 234 (1993) 779–815.
[24] W.L. DeLano, in: S. C. C. U. DeLano Scientific (Ed.), The PyMOL Molecular Graphics System, 2002, (http://www.pymol.org).
[25] A. Rafaeli, R. Bober, L. Becker, M.Y. Choi, E.J. Fuerst, R. Jurenka, Spatial distribution and differential expression of the PBAN receptor in tissues of adult *Helicoverpa* spp. (Lepidoptera: Noctuidae), Insect Mol. Biol. (2007) 287–293.
[26] C.J. Vankoppen, N.M. Nathanson, Site-directed mutagenesis of the M2 muscarinic acetylcholine-receptor — analysis of the role of N-glycosylation in receptor expression and function, J. Biol. Chem. 265 (1990) 20887–20892.
[27] M.M. Rosenkilde, T.N. Kledal, T.W. Schwartz, High constitutive activity of a virus-encoded seven transmembrane receptor in the absence of the conserved DRY motif (Asp-Arg-Tyr) in transmembrane helix 3, Mol. Pharmacol. 68 (2005) 11–19.
[28] M.Y. Choi, R.A. Jurenka, Site-directed mutagenesis and PBAN activation of the *Helicoverpa zea* PBAN-receptor, FEBS Lett. 584 (2010) 1212–1216.
[29] P.S. Stern, L. Yu, M.Y. Choi, R.A. Jurenka, L. Becker, A. Rafaeli, Molecular modeling of the binding of pheromone biosynthesis activating neuropeptide to its receptor, J. Insect Physiol. 53 (2007) 803–818.
[30] M. Pellegrini, D.F. Mierke, Molecular complex of cholecystokinin-8 and N-terminus of the cholecystokinin a receptor by NMR spectroscopy, Biochemistry 38 (1999) 14775–14783.
[31] M.Y. Choi, E.J. Fuerst, A. Rafaeli, R. Jurenka, Role of extracellular domains in PBAN/pyrokinin GPCRs from insects using chimera receptors, Insect Biochem. 37 (2007) 296–306.
[32] J.M. Lee, J.J. Hull, T. Kawai, K. Tsuneizumi, M. Kurihara, M. Tanokura, K. Nagata, H. Nagasawa, S. Matsumoto, Establishment of Sf9 transformants constitutively expressing PBAN receptor variants: application to functional evaluation, Front. Endocrinol. (Lausanne) 3 (2012) 1–8, (Article 56).
[33] G. Cazzamali, M. Torp, F. Hauser, M. Williamson, C.J.P. Grimmelikhuijzen, The *Drosophila* gene CG9918 codes for a pyrokinin-1 receptor, Biochem. Biophys. Res. Commun. 335 (2005) 14–19.
[34] T. Homma, K. Watanabe, S. Tsurumaru, H. Kataoka, K. Imai, M. Kamba, T. Niimi, O. Yamashita, T. Yaginuma, G protein-coupled receptor for diapause hormone, an inducer of *Bombyx* embryonic diapause, Biochem. Biophys. Res. Commun. 344 (2006) 386–393.
[35] C. Rosenkilde, G. Cazzamali, M. Williamson, F. Hauser, L. Sondergaard, R. DeLotto, C.J.P. Grimmelikhuijzen, Molecular cloning, functional expression, and gene

silencing of two *Drosophila* receptors for the *Drosophila* neuropeptide pyrokinin-2, Biochem. Biophys. Res. Commun. 309 (2003) 485–494.

[36] S.S. Olsen, G. Cazzamali, M. Williamson, C.J.P. Grimmelikhuijzen, F. Hauser, Identification of one capa and two pyrokinin receptors from the malaria mosquito *Anopheles gambiae*, Biochem. Biophys. Res. Commun. 362 (2007) 245–251.

[37] R. Predel, C. Wegener, Biology of the CAPA peptides in insects, Cell. Mol. Life Sci. 63 (2006) 2477–2490.

[38] L. Roller, N. Yamanaka, K. Watanabe, I. Daubnerova, D. Zitnan, H. Kataoka, Y. Tanaka, The unique evolution of neuropeptide genes in the silkworm *Bombyx mori*, Insect Biochem. Mol. Biol. 38 (2008) 1147–1157.